iTOUGH2 GLOBAL SENSITIVITY ANALYSIS MODULE: APPLICATIONS TO CO_2 STORAGE SYSTEMS

Haruko M. Wainwright, Stefan Finsterle, Yoojin Jung, Quanlin Zhou, Jens T. Birkholzer

Lawrence Berkeley National Laboratory
1 Cyclotron Road
Berkeley, CA, 94720, USA
e-mail: hmwainwright@lbl.gov

ABSTRACT

We have implemented a global sensitivity analysis module into iTOUGH2. While a *local* sensitivity analysis perturbs parameters from a single set of reference values and computes the derivative of system responses, a *global* sensitivity analysis explores the entire parameter space, providing more robust sensitivity measures as well as identifying the presence of nonlinearity in system responses and interactions among parameters. The new module includes two global sensitivity methods: the Morris and Saltelli methods.

To demonstrate this new capability, we coupled this module with two forward models related to CO_2 sequestration: (1) a high-resolution reservoir-scale model for a hypothetical CO_2 storage project and (2) an analytical model for computing the transient head change induced by injection/ extraction/ leakage through multiple wells in a multilayered system. Our results illustrate the characteristics of each sensitivity method. The local sensitivity is sufficient to identify dominant parameters and useful for understanding the system. The Morris method can identify nonlinear/interaction effects as well as provide more robust sensitivity measures with relatively small computational cost. The Saltelli method can provide more rigorous and quantitative sensitivity measures in the context of uncertainty quantification, although it comes at a high computational cost.

INTRODUCTION

iTOUGH2 (Finsterle, 2010) has been developed first as an inverse modeling and parameter estimation (PE) tool for hydrogeological applications, which works with the TOUGH2 flow and transport simulators as well as other simulators through the PEST protocol. Various modules have been implemented, such as the uncertainty analysis module for Monte-Carlo simulations, the coupled hydrogeological-geophysical inversion module, and various other tools.

Many studies (e.g., Finsterle et al., in press) have identified essential tools for hydrological modeling under uncertainty, and also for real-world hydrological projects that start from site characterization and lead to prediction. They include parameter estimation, uncertainty analysis (UA), sensitivity analysis (SA), data-worth analysis, and experimental design. With the first two already implemented and tested intensively, we consider iTOUGH2 to be one of the most effective, comprehensive tools for model development and analysis.

The ability to support a formal sensitivity analysis is a key component in such a software tool, since there is a strong interaction between SA and other components of the workflow. Identifying sensitive or important parameters is critical (1) to check whether a given dataset has sufficient information to determine a parameter given the uncertainty of other parameters in PE, (2) to identify the most effective data locations and timing in the experimental design, (3) to determine how to allocate limited resources for estimating each parameter as part of a data-worth analysis, and (4) to reduce the number of parameters to be varied/estimated and hence to reduce the computational burden in PE and UA.

In addition, we believe that the SA tool can be used not only for selecting the important parameters, but also for improving the understanding of the system. For example, identifying the positive or negative effects of each parameter

will be important for determining safety margins in engineering systems. The time profile of sensitivity can identify which parameter influences the model output at which time period. We can also identify interactions among parameters.

In the iTOUGH2 SA module, we have, in addition to the existing local sensitivity method, implemented two global sensitivity methods—that of Morris (Morris, 1991) and Saltelli (Saltelli et al., 2008). These global methods provide more robust sensitivity measures as well as identify the nonlinearity in system responses and interactions among parameters.

The objectives of this study are to (1) introduce the global-sensitivity-analysis methods, (2) compare the three sensitivity methods in terms of interpretation and computational cost. To demonstrate the utility of the iTOUGH2 sensitivity analysis module, we used two hydrological problems related to CO_2 sequestration: a high-resolution basin-scale model for a hypothetical storage project (using TOUGH-MP) and an injection/leakage-induced pressure model (using an analytical solution). Since the latter model is computationally inexpensive, we use it to explore the computational cost of the Morris method in more detail.

METHODOLOGY

In this section, we introduce the global sensitivity methods. Although each method is documented in detail in Morris (1991) and Saltelli et al. (2008), we describe them briefly here for completeness. We denote a set of parameters by $\{x_i|\ i=1,\ldots,k\}$ (the number of parameters is k) and a scalar output of a model by y, which is a function of $\{x_i\}$; $y = f(\{x_i\})$.

Local Sensitivity Method

The local sensitivity is defined as a partial derivative, i.e., the change in an output variable caused by a unit change in each parameter from the reference value. When we have a numerical model, we can compute the derivative by changing each parameter by a small increment Δx_i from the reference parameter values x_i^* and computing the difference in the output. The scaled sensitivity is the derivative scaled by the standard deviation of parameters and measurement errors. The scaled, dimensionless sensitivity is defined as:

$$S_i^{local} = \frac{\sigma_x}{\sigma_y}\left.\frac{\partial y}{\partial x_i}\right|_{x_i^*} = \frac{\sigma_x}{\sigma_y}\frac{f(x_1^*,..,x_i^*+\Delta x_i,..) - f(x_1^*,..,x_i^*,..)}{\Delta x_i}$$

where σ_x is the standard deviation of the parameter, and σ_y is the standard deviation of the model output, reflecting its measurement error or acceptable mean residual in an inversion.

Morris Sensitivity Method

In the Morris one-at-a-time (OAT) method (Morris, 1991), the parameter range— normalized as a uniform distribution in [0, 1]—is partitioned into (p–1) equally sized intervals, so that each parameter takes values from the set {0, 1/(p–1), 2/(p–1), …, 1}. From the reference point of each parameter randomly chosen from the set {0, 1/(p–1), 2/(p–1), …, 1– Δ}, the fixed increment $\Delta = p/\{2(p-1)\}$ is added to each parameter in a random order to compute the elementary effect (EE) of each parameter, which is the difference in output y caused by the change in the respective parameter. k+1 runs are necessary to complete one path, which is to change each parameter once from one set of reference values. By having multiple paths (i.e., multiple sets of reference parameter values and multiple, random orders for changing each parameter), we have an ensemble of EEs for each parameter. We can compute three statistics: the mean of EE, the variance in EEs, and the mean of absolute EEs (mean of |EE|). The mean EE can be regarded as a global sensitivity measure, and is used to identify noninfluential factors. The variance of EEs is used to compute the standard error of mean (SEM) for identifying nonlinear or interaction effects.

Saltelli Sensitivity Method

While the local and Morris sensitivity is difference-based, the Saltelli method is variance-based. Saltelli et al. (2008) defined the sensitivity by $\mathbf{V}[\mathbf{E}[Y|X_i]]/\mathbf{V}[Y]$ for parameter importance, where $\mathbf{E}[\bullet]$ and $\mathbf{V}[\bullet]$ represent mean and variance, respectively. Conceptually, this measure quantifies the contribution of each parameter to the uncertainty of the output. In addition, Saltelli et al. (2008) defined the total sensitivity by $\mathbf{V}[\mathbf{E}[Y|X_{-i}]]/\mathbf{V}[Y]$, where $\mathbf{E}[Y|X_{-i}]$ represents the mean of Y conditioned on all the

parameters but X_i. The total sensitivity is used to identify unimportant parameters. We can compute these two measures–sensitivity and total sensitivity–using the Monte-Carlo integration described in Saltelli (2008).

DEMONSTRATION PROBLEM SETUP

Reservoir-scale CO_2 Migration Problem

The reservoir-scale CO_2 migration model was developed based on a geological study in the Southern San Joaquin Basin, California, using the datasets obtained at many oil fields in that region (Birkholzer et al., 2011; Zhou et al., 2011; Zhou and Birkholzer, 2011). The domain includes 12 discontinuous or continuous formations, extending 84 km in the eastern direction and 112 km in the northern direction. The domain also includes several faults, which are known to be near-impermeable sealing faults at large depth.

The Vedder Formation—considered as the injection formation—dips upward towards a shallow outcrop area located along the eastern model boundary, at an average slope of 7 degree. The overlying Temblor-Freeman Shale (TF Shale) is considered a suitable caprock for stratigraphic containment of the injected super-critical CO_2. We also consider six alternating sand/shale layers—Vedder Sand (V Sand) and Vedder Shale (V Shale)—in the Vedder Formation, based on the datasets. At the injection well, the Vedder Formation is 400 m thick, and its top elevation is -2,751 m. The cap rock (TF Shale) is about 200 m thick. The plan view of the Vedder Formation is shown in Figure 1(a).

We used the massively parallel version of TOUGH2 (Zhang et al., 2008) with the ECO2N module to simulate injection and migration of supercritical CO_2 in the brine system. The simulation time includes an injection period of 50 years with an injection rate of 5 Mt per year, and a post-injection period of 150 years. In this study, the 3D mesh consists of 64,214 elements, the number of which falls in between that of the fine mesh (Zhou et al., 2010; Zhou and Brikholzer (2011) and that of the coarse mesh used in Birkholzer et al. (2011). Figure 1(b) shows the plan view of the numerical mesh.

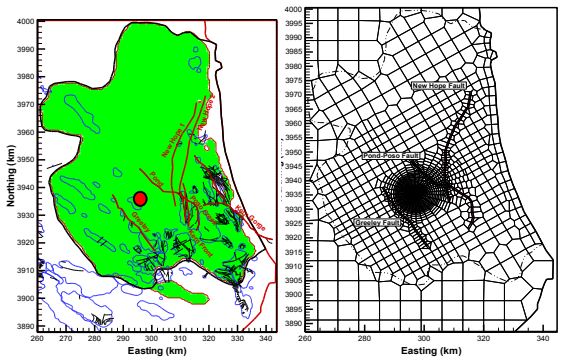

(a) (b)

Figure 1. (a) Plan view of the Vedder formation and the faults, and (b) Plan view of the numerical domain with mesh. The red dot is the injection location.

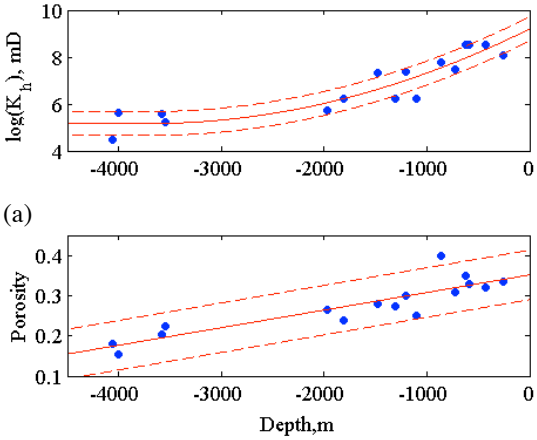

(a)

(b)

Figure 2. Estimated depth-dependent (a) V Sand permeability and (b) V Sand porosity. The blue dots are the data values, the solid red line is the estimated parameter value, and the dotted read lines are the uncertainty bounds (± two standard deviations).

In our SA, we varied five properties (permeability, porosity, pore compressibility, van Genuchten α and m) of three geological units (V Sand, V Shale, TF Shale), so that we have a total of 15 parameters. For the V Sand permeability and porosity, we estimated the depth-dependent parameter values and their uncertainty ranges using the available datasets (Figure 2). For the rest of the parameters, the reference parameter values are shown in Table 1. The range of parameters in this study is one order of magnitude in permeability, a factor of five in pore compressibility, 30% in porosity and van

Genuchten m, and half an order of magnitude in van Genuchten α. As performance measures, we consider various system responses, such as CO_2 saturation and pressure buildup at various locations, and CO_2 plume extent. For demonstration purposes, we chose one performance measure; CO_2 saturation (S_{CO2}) at 1.78 km east from the injection point.

Table 1. Reference parameter values: horizontal permeability k_h, anisotropy ratio k_v/k_h, porosity Φ, pore compressibility β_p, van Genuchten α and m

	TF Shale	V Sand	V Shale
k_h, mD	0.002	*dep-dep.	0.1
k_v/k_h	0.5	0.2	0.5
Φ	0.338	*dep-dep.	0.32
β_p,10^{-10}, Pa^{-1}	14.5	4.9	14.5
α, 10^{-5}, Pa^{-1}	0.42	13	0.42
m	0.457	0.457	0.457

* Depth-dependent values shown in Figure 2.

Leakage-Induced Pressure Problem

A semi-analytical model was developed by Cihan et al. (2011) to describe the transient pressure changes caused by injection or extraction activities in a multilayered aquifer system. It models flow through aquitards (diffusive flow or diffusive leakage) as well as flow through the leaky wells (focused flow or focused leakage). In the CO_2 storage system, this model has been used to predict the pressure disturbance caused by the CO_2 injection. Also, this model has become the basis for developing a system to detect possible CO_2 leakage through wells or faults, since the pressure propagates much faster than the CO_2 plume. (We refer to Cihan et al. (2011) for a more detailed description and a discussion of the assumptions.)

In this study, we consider a three-layered system that consists of the reservoir (injection layer), the aquitard, and an upper aquifer, as shown in Figure 3. Each layer is assumed to be a homogenous and isotropic medium with uniform thickness and infinite extent. We also assume that the leaky well is 2000 m away from the injection point.

In SA, we perturbed the following parameters: hydraulic conductivity K and storativity S for the reservoir, the aquitard and the aquifer, and the hydraulic conductivity of the leaky well. The total number of parameters is seven. Reference parameter values are shown in Table 2. The parameter range is one order of magnitude in hydraulic conductivity, and a factor of five in storativity. As a performance measure, we are interested in the pressure buildup at a fixed point in the overlying aquifer, which corresponds to the leaky well location.

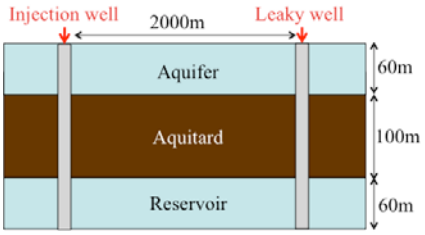

Figure 3. Conceptual model setup for the pressure leakage problem.

Table 2. Reference parameter values: hydraulic conductivity K and storativity S

	Aquifer	Aquitard	Reservoir	Well
K, m/s	2.00E-1	2.00E-6	2.00E-1	2.00E+5
S, 1/m	1.88E-6	1.47E-6	1.88E-6	N/A

RESULTS AND DISCUSSION

Reservoir-scale CO_2 Migration Problem

Local sensitivity

The local sensitivity was computed using 16 simulations. Figure 4(a) shows the time series of local sensitivity for CO_2 saturation (S_{CO2}) at a fixed point. There are three dominant parameters: V Sand permeability, porosity and van Genuchten m. All three curves have two spikes, which correspond to the plume arrival and departure. Higher permeability and m lead to higher plume/brine mobility, which leads to positive sensitivity at the plume arrival (i.e., earlier arrival and higher S_{CO2}) and negative sensitivity at plume departure (i.e., earlier departure and lower S_{CO2}). The large porosity means there is more brine to be displaced at the arrival and more CO_2 at the departure, so that porosity has the opposite effect of permeability and m.

The pore-size distribution index m has a large impact at the arrival but not at the departure. This is attributed to the specific implementation

of the two-phase model in the current version of TOUGH2-MP, which uses the van Genuchten model for relative brine permeability (k_{lr}) and capillary pressure, and the Corey model for relative gas permeability—so that the relative gas permeability does not depend on m (Pruess et al., 1999). Since the derivative of relative brine permeability with respect to m ($\partial k_l/\partial m$) increases in absolute magnitude towards full brine saturation, m is more influential near full brine saturation and hence at plume arrival. This result may change once the full van Genuchten model and the hysteresis model (Doughty, 2007) are implemented in TOUGH2-MP, which makes m dependent on gas relative permeability. The point to address here is that the sensitivity analysis is useful in identifying and understanding an effect that is potentially an artifact of model implementation.

CO_2 saturation at other locations (not shown here) also had similar profiles and showed significant sensitivities to the same three parameters. This result may support the development of simple analytical or semi-analytical solutions, or decoupled reservoir-only CO_2 migration models. For example, we found that the van Genuchten α has a negligible effect on far-field CO_2 saturation, consistent with some of the analytical studies that neglect the capillary pressure (e.g., Nordbotten et al., 2009). We also note that this conclusion is applicable only to the CO_2 saturation; we observed significant sensitivity of pressure buildup to other parameters, such as V Sand pore compressibility and TF Shale permeability.

Morris sensitivity

In the Morris method, the EEs were computed by four partitions and ten paths. The total number of simulations was 160. Figure 4(b) shows the time profile of mean EE from the Morris method. Compared to the local sensitivity in Figure 4(a), the spikes are smoothed out over time, since the plume arrival/departure time is more distributed. In terms of importance ranking and sign of effects, we draw a conclusion similar to the local sensitivity analysis, with the same three parameters being identified as most influential. However, there are some differences from the local sensitivity: the porosity effect is more prominent at early times, and the V Sand permeability becomes dominant in the post-injection period.

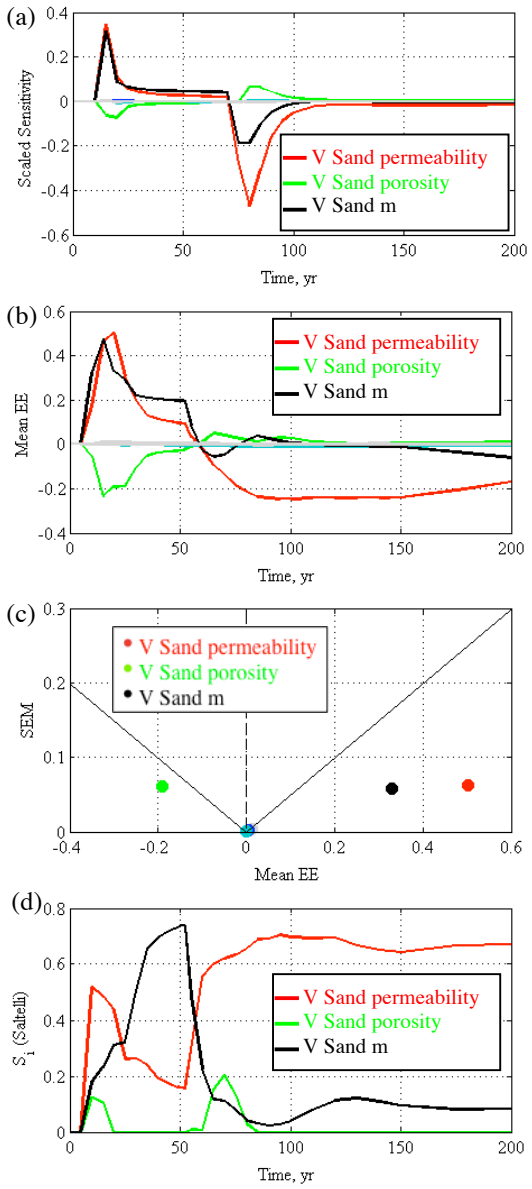

Figure 4. SA results for the reservoir-scale CO_2 migration problem: (a) time profile of the local sensitivity, (b) time profile of the Morris mean EE, (c) crossplot of Mean EE and SEM of S_{CO2} at 20 years from the Morris method, and (d) time profile of Saltelli sensitivity. In (c), the solid black lines correspond to (Mean EE) = ± 2SEM.

Figure 4(c) shows the cross-plot of mean EE and standard error of mean (SEM) at one time (20 years). In this figure, parameters with higher SEM, i.e., those that are closer to the grey solid lines (Mean EE = ±2SEM) exhibit stronger nonlinearity or interaction effects. The reservoir

permeability and *m* have large mean EE and low SEM values; the porosity is close to the black line, indicating nonlinearity or interaction effects. In general, we observe that the parameters with higher SEM have different interpretations or importance rankings between the local and global sensitivity analyses.

Saltelli sensitivity

Based on the Morris method, we chose five parameters for the Saltelli sensitivity (V Sand permeability, porosity, compressibility, *m*, and TF Shale permeability). We computed the Saltelli sensitivity using 840 realizations. Figure 4(d) shows the time profile of Saltelli sensitivity. The sensitivity is normalized by the variance at each time slice, so that there are no peaks such as those that appeared in the Morris sensitivity in Figure 4(b). The sum of the sensitivity of each parameter, however, does not become one, since there exist nonlinear or interaction effects (Saltelli, 2008).

Based on this figure, the V Sand van Genuchten *m* accounts for about 70% of the total variability of the output at time 30–50 years, and the V Sand permeability accounts for about 70% after 100 years (most of the post-injection period). The qualitative interpretation and ranking, however, are the same as the Morris mean EE.

Leakage-Induced Pressure Problem

Local sensitivity

In the same manner as in the reservoir model, the time profile for scaled sensitivity is plotted in Figure 5(a) for 10 years and (b) for 1 year.

In Figure 5(a), we can see that the aquifer and reservoir *K* is influential, while the sensitivity to the aquitard *K* increases as the diffusive leakage reaches the shallow aquifer. The hydraulic conductivity of the leakage pathways—the well *K* and aquitard *K* at later times—have a positive impact, whereas the aquifer and reservoir *K*s have a negative impact; the higher *K* dissipates and reduces the pressure buildup, except for pressures along the leakage pathways.

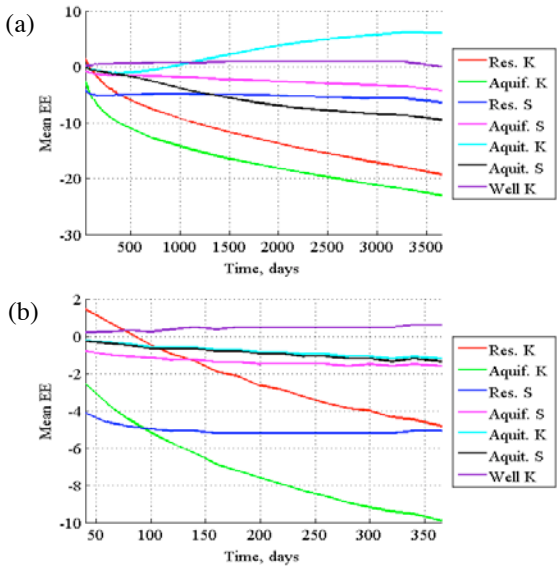

Figure 5. Local sensitivity results for the pressure leakage problem.

In Figure 5(b), however, we can see that the reservoir *K* has a positive effect at the beginning. This is because the reservoir *K* contributes to pressure propagation through the system, and the higher reservoir *K* produces faster arrival of the pressure buildup at this observation point. The reservoir *S* has a relatively large effect at the beginning, since the compressible matrix pores absorb the initial pressure increase.

Morris sensitivity

Figure 6 shows the mean EE from the Morris method. Although the magnitude is different, it gives a fairly consistent interpretation compared to the local sensitivity method, except that (1) the sensitivity to the aquitard *S* becomes smaller relative to the other parameters, and (2) the sensitivity to the reservoir *S* increases at early times. This is considered to be an interaction effect, since hydraulic conductivity and storativity have a nonadditive impact on pressure buildup.

Figure 7 shows the mean EE of the aquitard *K* and reservoir *K* at 10 years as a function of the number of paths with different numbers of partitions *p*. As expected, there are considerable fluctuations in the estimated EE if only a few paths are evaluated. After about 100 paths, the estimate appears stabilized. Note that evaluating 100 paths is generally unfeasible for a computationally expensive simulation model. Running

fewer paths still provides some useful information on the relative importance of a parameter, making the Morris approach a viable tool for global sensitivity analysis.

The number of partitions has little impact on the mean EE in this case. We note that increasing the number of partitions tends to systematically reduce mean EE, an effect that requires further analysis, but that seems likely to be related to the nature of nonlinearity and its evaluation using a decreasing perturbation Δ.

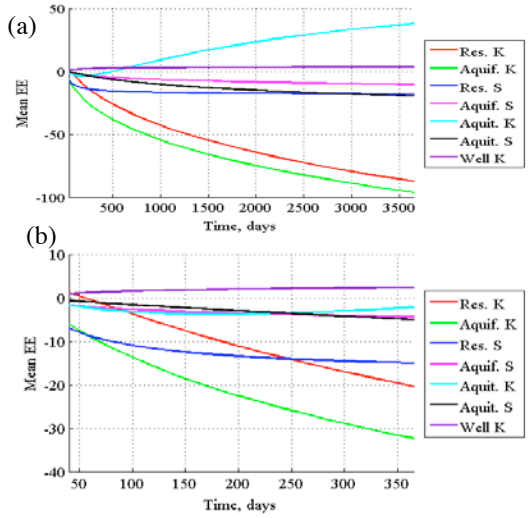

Figure 6. Morris sensitivity results for the pressure leakage problem.

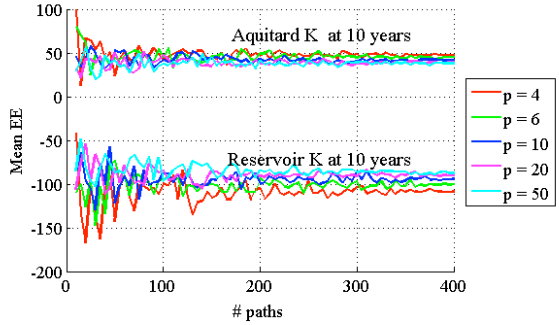

Figure 7. Mean EE of the aquitard *K* and reservoir *K* as a function of the number of paths with different numbers of partitions *p*

Figure 8 shows the crossplot of the mean EE and STD for the reservoir *K*, reservoir *S* and aquitard *K* with different number of paths (*n*). The reservoir *K* has a large effect compared to the reservoir *S* and aquitard *K*. The dots are converged at 200-400 paths, although 10 paths are enough to compare the importance of these three parameters qualitatively; for example, the reservoir *K* has a large mean EE with relatively smaller STD. Since SEM decreases as the number of paths increases, the line for Mean EE = ± 2SEM changes with the number of paths. The effect of aquitard *K*, for example, is not significant with *n*=10 (above the line), but it is significant at *n*=400 (below the line). With the Morris method, we can determine whether the effect is significant or not, with nonlinearity/interaction effects as well as with a limited number of runs.

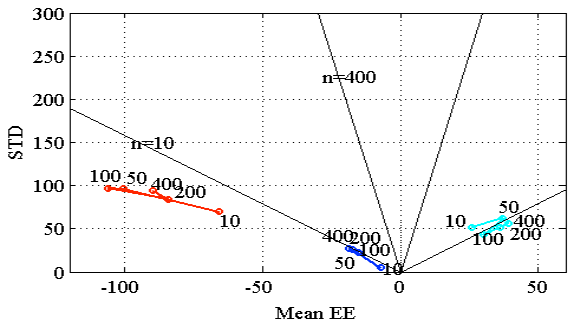

Figure 8. Mean EE vs. STD for the reservoir *K* (red), reservoir *S* (blue) and aquitard *K* (light blue) with different number of paths (10, 50, 100, 200,400). *p* = 20. The black lines correspond to Mean EE = ± 2SEM.

CONCLUSIONS

In this study, we have introduced the new global sensitivity analysis (SA) tool of iTOUGH2. We have shown that the SA tool can be used not only for selecting the important parameters, but also for better understanding systems.

Using the reservoir-scale CO_2 migration model, we compared three SA methods. The results showed that the three sensitivity methods give similar interpretations and importance rankings, except when a parameter has a strong nonlinear effect or interacts with some other parameters—which is the case when a global SA is warranted. We have found that the local sensitivity is sufficient in our cases to identify the influential parameters. Even for cases with nonlinear or interaction effects, the local sensitivity is still useful in improving system understanding (e.g., the high sensitivity of plume arrival/departure to parameters affecting CO_2 mobility) and helps interpret the results from the Morris or Saltelli methods. The Morris sensitivity method provides many uses (e.g., it can identify positive or negative effects, select influential parameters, suggest the presence of nonlinear or interaction effects) with relatively small computational

burden. The Saltelli sensitivity method gives more rigorous/quantitative sensitivity measures, although it is computationally expensive.

With our semi-analytical pressure leakage model, we have explored the computational cost of the Morris method in more detail, in addition to comparing the local and Morris methods. In the Morris method, increasing the number of partitions did not change the mean EE of parameters significantly. Using the crossplot of mean EE and STD, we found that increasing the number of paths has a small effect on the estimation of EE, i.e., the relative importance of a parameter can be evaluated using a relatively small number of simulation runs. The Morris method also allows us to tell the significance of sensitivity measures (e.g., Mean EE) under non-linearity or interactions as well as a limited number of runs. Finally, this study has shown that incorporating global-sensitivity analysis methods into iTOUGH2 strengthens the code's overall value as a model development, experimental design, and data analysis tool.

ACKNOWLEDGMENT

The authors wish to thank to Jeff Wagoner for developing the geologic framework model of the Southern San Joaquin Basin. This work was funded by the Assistant Secretary for Fossil Energy, National Energy Technology Laboratory (NETL), National Risk Assessment Partnership (NRAP), of the U.S. Department of Energy under Contract No. DE-AC02-05CH11231.

REFERENCES

Birkholzer, J.T., Q. Zhou, A. Cortis and S. Finsterle, A sensitivity study on regional pressure buildup from large-scale CO2 storage projects, *Energy Procedia*, 4:4371-4378, 2011

Birkholzer, J.T., A. Cihan, Q. Zhou, Impact-driven pressure management via targeted brine extraction—Conceptual studies of CO_2 storage in saline formations, Int. J. of Greenhouse Gas Control, 7, 168-180, 2012.

Cihan, A., Q. Zhou and J.T. Birkholzer, Analytical solutions for pressure perturbation and fluid leakage through aquitards and wells in multilayered aquifer systems, *Water Resour Res.*, W10504, 2011.

Doughty C. Modeling geologic storage of carbon dioxide: comparison of non-hysteretic and hysteretic characteristic curves, *Energy Conversion and Management*, 48(6), 1768-1781, 2007.

Finsterle, S., *iTOUGH2 User's Guide*, Report LBNL-40040, Lawrence Berkeley National Laboratory, Berkeley, Calif., 2010.

Finsterle, S., M.B. Kowalsky, and K. Pruess, TOUGH: Model Use, Calibration and Validation, *Transaction of the American Society of Agricultural and Biological Engineers*, in press.

Jung, Y., Q. Zhou, and J.T. Birkholzer, Joint inversion of pressure-based observation data for early detection of brine or CO2 leakage through high-permeability pathways, Ground Water, 2012 (in preparation).

Morris, M.D., Factorial Sampling Plans for Preliminary Computational Experiments, *Technometrics*, 33(2):161-174, 1991.

Nordbotten, J. M., D. Kavetski, M. A. Celia, and S. Bachu, Model for CO2 Leakage Including Multiple Geological Layers and Multiple Leaky Wells, *Environ. Sci. and Technol.*, 43 (3), 743-749, 2009

Pruess, K., C. Oldenburg, and G. Moridis, *TOUGH2 User's Guide, Version 2.0*, Report LBNL-43134, Lawrence Berkeley National Laboratory, Berkeley, Calif., 1999.

Saltelli, A., Ratto, M., Andres, T., Campolongo, F., Cariboni, J., Gatelli, D., Saisana, M., Tarantola, S., Global Sensitivity Analysis: The Primer, John Wiley and Sons, 2008

Zhang, K., Wu, Y.S., Pruess, K., 2008. *User's Guide for TOUGH2-MP – A Massively Parallel Version of the TOUGH2 Code*. Report LBNL-315E, Lawrence Berkeley National Laboratory, Berkeley, CA, USA.

Zhou, Q., J.T. Birkholzer, and J.L. Wagoner, Modeling the potential impact of geologic carbon sequestration in the southern San Joaquin basin, California, The Ninth Annual Carbon Capture & Sequestration, Pittsburgh, PA, May 2011.

Zhou, Q., and J.T. Birkholzer, On scale and magnitude of pressure build-up induced by large-scale geologic storage of CO2, Greenhouse Gases: Science and Technology, 1,11-20 2011.